Rapid Communication

J. Biochem. **140**, 305–311 (2006)
doi:10.1093/jb/mvj172

Structural Basis for Induced-Fit Binding of Rho-Kinase to the Inhibitor Y-27632

Hiroto Yamaguchi[1,2,*], Yukiko Miwa[1,*], Miyuki Kasa[1,2], Ken Kitano[1], Mutsuki Amano[3], Kozo Kaibuchi[3] and Toshio Hakoshima[1,2,†]

[1]Structural Biology Laboratory, Nara Institute of Science and Technology, and [2]CREST, Japan Science and Technology Agency, Keihanna Science City, Nara 630-0192; and [3]Department of Cell Pharmacology, Nagoya University, Graduate School of Medicine, 65 Tsurumai, Showa, Nagoya 466-8550

Received June 7, 2006; accepted July 15, 2006

Rho-kinase is a main player in the regulation of cytoskeletal events and a promising drug target in the treatment of both vascular and neurological disorders. Here we report the crystal structure of the Rho-kinase catalytic domain in complex with the specific inhibitor Y-27632. Comparison with the structure of PKA bound to this inhibitor revealed a potential induced-fit binding mode that can be accommodated by the phosphate binding loop. This binding mode resembles to that observed in the Rho-kinase-fasudil complex. A structural database search indicated that a pocket underneath the phosphate-binding loop is present that favors binding to a small aromatic ring. Introduction of such a ring group might spawn a new modification scheme of pre-existing protein kinase inhibitors for improved binding capability.

Key words: drug design, protein flexibility, protein kinase, specificity.

Rho-kinase (ROKα, Rho-associated kinase or $p160^{ROCK}$) (*1–4*) is a serine/threonine protein kinase that is one of the best characterized targets of the activated RhoA molecule. Rho-kinase has an isozyme (ROKβ/ROCK I) that exhibits 92% sequence identity in the catalytic domain and belongs to the AGC family of eukaryotic protein kinases whose members include PKA and PKC. These kinases contain a protein kinase domain that requires a C-terminal extension outside the catalytic core domain for catalytic activity that contains the so-called 'hydrophobic motif' of six residues, FXXF[T/S][F/Y] (where X stands for any amino acid residue) (*5–7*). Unlike the AGC kinases, Rho-kinase possesses not only an important C-terminal extension, but a novel N-terminal extension required for catalytic activity, features apparent when initially identified as an activated RhoA target (*8*).

Aberration of the Rho-kinase pathway involved in actomyosin contraction processes can have serious pathophysiological consequences. Abnormal contraction of vascular smooth muscle causes diseases such as hypertension and vasospasm of the coronary and cerebral arteries (*9*). This has been observed in various neurological disorders in the central nervous system (*10*). Several specific inhibitors of Rho-kinase have been developed for treating these diseases and for analyzing cellular events. The therapeutic potential of Rho-kinase inhibitors is reflected in their ability to induce significant vasodilatory effects (*11*). Currently, two major series of Rho-kinase inhibitors are widely used: isoquinoline derivatives and 4-aminopyridine derivatives. One of the most prominent isoquinoline derivatives is fasudil (HA-1077), and is currently used to clinically treat cerebral vasospasm (*12*). The 4-aminopyridine derivative Y-27632 (*13*) displayed an encouraging selectivity profile toward Rho-kinase in an experiment that compared its binding to 25 protein kinases (*14*). Y-27632 is representative of the series that is most widely utilized in biological and pharmacological experiments (*10*).

Previously, we determined the Rho-kinase-fasudil complex structure and revealed an induced-fit conformational change in the drug binding site (*15*). This observation prompted us to examine the Rho-kinase structure bound to the specific inhibitor Y-27632. Here, we report the crystal structure of the kinase domain of Rho-kinase in complex with the specific inhibitor Y-27632.

A 400-residue Rho-kinase fragment (residues 18–417) was expressed in Sf9 insect cells with a hexa-histidine tag using the Bac-to-Bac recombinant baculovirus expression system (Life Technologies) and the protein was purified as described previously (*15*). 5.3 mg of purified protein was obtained from 60 g wet cells, and the purified protein was concentrated prior to crystallization experiments. Crystals were initially obtained by vapor diffusion at 20°C in 1–5 μl hanging drops that contained equal volumes of a cocktail solution of 7.8 mg/ml protein and 1 mM inhibitor Y-27632, and a reservoir solution consisting of either sodium citrate, ammonium sulfate, PEG6K or PEG8K as a precipitating reagent. Multiple rounds of macro seeding were required to obtain isolated monolithic crystals with increased thickness. Hexagonal rod-shaped crystals were obtained from hanging drops with a reservoir solution containing 0.9 M sodium citrate, 0.1 M Tris-HCl (pH 8.0) and 6.3 mM FOS-Choline-9. All data sets were measured from frozen crystals cryoprotected in 20% (w/v) glycerol. A preliminary data set was collected at home using an R-AXIS VII area detector mounted on an FR-E X-ray generator (RIGAKU). Judged from the merging statistics and systematic absences, the crystals belong to a primitive hexagonal space group, either $P6_222$ or $P6_422$. A data set for structure determination and refinement was collected on DIP6040 imaging plates (Bruker-AXS) at the synchrotron

†To whom correspondence should be addressed. Tel: +81-743-72-5570, Fax: +81-743-72-5579, E-mail: hakosima@bs.naist.jp
*These authors contributed equally to this work.

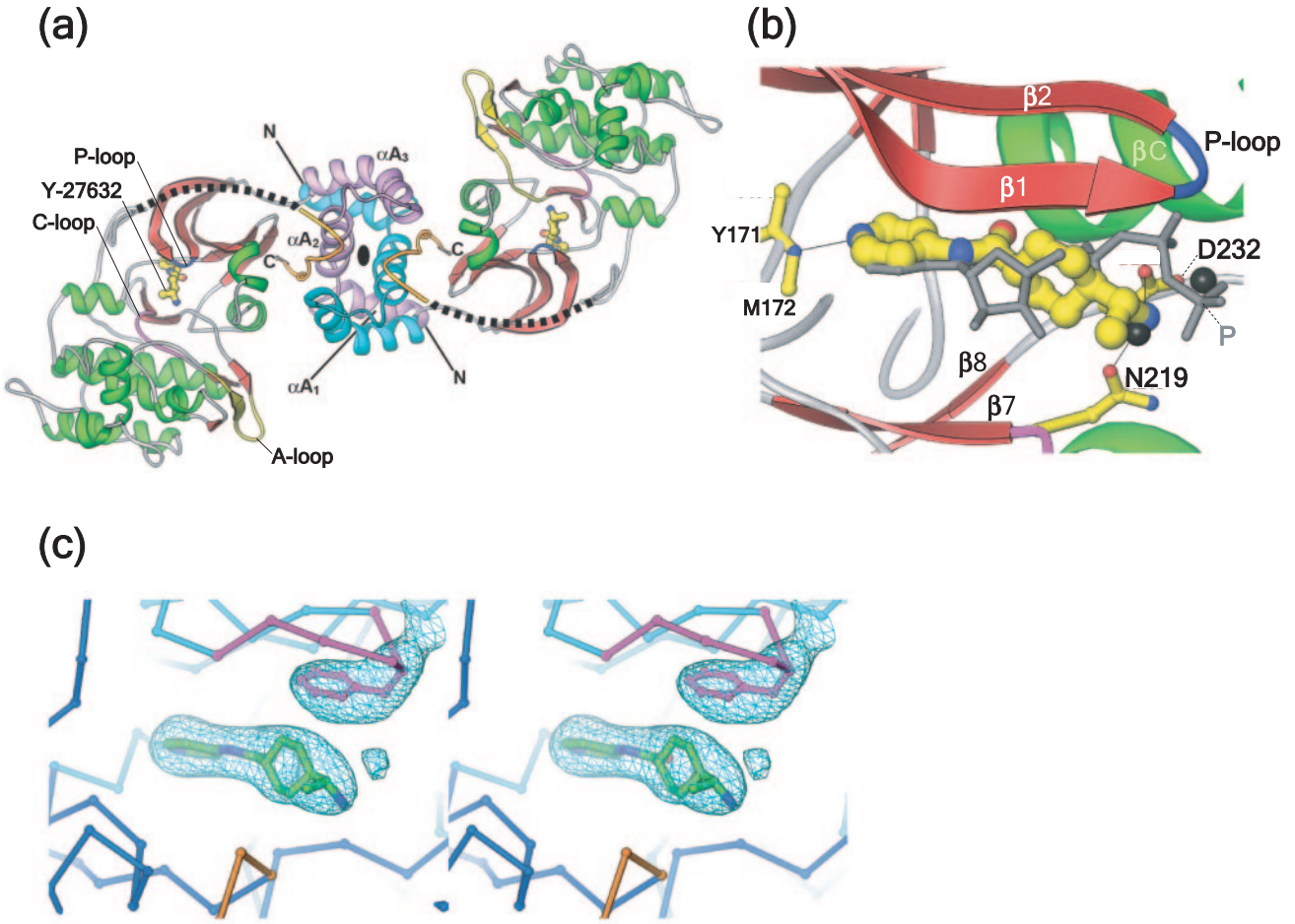

Fig. 1. **Structure of the Rho-kinase-Y-27632 complex.** (a) Ribbon diagram showing the overall dimer structure. The crystallographic dyad that relates two monomers is shown as a black oval in the center. Three helices (αA_1, αA_2 and αA_3) of the N-terminal extension are labeled for one monomer (pink), and colored separately for two protomers in pink and cyan. The C-terminal extension (residues 399–417) is colored orange. Helices and β-strands in the catalytic core are colored green and red, respectively. The phosphate binding loop (P-loop), the catalytic loop (C-loop), and the activation loop (A-loop) are colored blue, magenta and yellow, respectively. The bound inhibitor Y-27632 is shown as a ball-and-stick model in the interlobal cleft. The segments (residues 389–398; broken lines) and the N-terminal seven residues (residues 18–24) were omitted in our structural model due to poor electron density. (b) A close-up view of the Y-27632 binding in the ATP binding cleft of Rho-kinase. The catalytic domain and the inhibitor are shown as in (a). The AMP-PNP molecule of PKA (PDB code: 1CDK) that is superposed on Rho-kinase is shown as a grey stick model. The associated magnesium ions are shown as black spheres. The main-chain bonds between residues 171 and 172 in addition to the side-chains of residues 219 and 232 are shown as ball-and-stick models, where polar interactions with the inhibitor are indicated by thin lines. (c) A close-up stereoview of the inhibitor Y-27632 bound to Rho-kinase. Electron density (countered at 2.5σ) was computed using ($2F_o$–F_c) coefficients and phases from a model obtained following simulated annealing with the inhibitor and the Phe103 side chain omitted.

beamline BL44XU at SPring-8 in Japan, and was processed and scaled using program suite HKL2000 (*16*) (Table 1). Crystallographic structure determination was carried out in a standard manner (*16–18*). The structure was determined by molecular replacement using Molrep (*17*) with our previously reported Rho-kinase-fasudil complex structure (*15*) as a search model and was then refined using REFMAC5 (*19*). The stereochemical quality of the model was monitored using the program PROCHECK (*20*). The final model contains no outlier in the Ramachandran plot defined by PROCHECK with 99.7% residues in the most favourable and additional allowed regions.

The structure revealed a functional dimer formed by head-to-head association of the N-terminal extension (residues 18–84) that folds into 3 helices (αA_1,αA_2, and αA_3) (Fig. 1a). Two αA_2 helices self-assemble through leucine zipper-like interactions around the crystallographic dyad axis, which exemplifies the hydrophobic nature of the dimer interface. The catalytic core domain shows the canonical protein kinase fold consisting of a smaller N-terminal lobe and a larger C-terminal lobe. The very end of the C-terminal extension (residues 399–417) is sandwiched between helix αA_2 and the N-terminal lobe of the catalytic domain.

In our crystal, Thr249 in the activation loop (A-loop), a putative phosphorylation site, is not phosphorylated, whereas the loop adopts in an extended conformation providing accessibility of the catalytic center for substrates. Similarly, another putative phosphorylation site, Thr414, located at the hydrophobic motif is not

Table 1. **Crystallographic data.**

Diffraction data[a]	
Wavelength (Å)	0.9000
Space group	$P6_122$
Unit cell (Å)	$a = b = 90.78$, $c = 341.28$
Resolution (Å)	30.0–3.10 (3.21–3.10)
Unique reflections	16,013
Redundancy	14.9
Completeness (%)	99.5 (99.9)
$I/\sigma(I)$	30.0 (9.8)
R_{sym} (%)	7.4 (23.6)
Refinement statistics[b]	
Atomic model	
Amino acid residues	383
Water molecules	8
Y-27632	1
Nonhydrogen atoms	3,120
Reflections used	15,995
R_{work} (%)	23.2
R_{free} (%)	27.7
Overall B factors (Å^2)	
Protein	61.1
Y-27632	50.3
Water molecules	41.8
All atoms	61.0
RMS deviations	
Bond length (Å)	0.016
Bond angles (°)	1.718
Main-chain B-factor (Å^2)	0.771

[a]Data for the outermost resolution shell are given in parentheses. Measurements were excluded from merging when $I/\sigma(I) < 0$.
[b]A subset of data (5%) was excluded from the refinement and used for the free R-value calculation.

phosphorylated either. Nonetheless, two lobes of the catalytic core domain are in a closed active form and the relative position of the key catalytic residues (Lys121, Glu140, Asp214, Asn219 and Asp232 in Rho-kinase) is consistent with that found in active protein kinases, with small rms C_α distances being less than 0.8 Å when compared with the active closed form of PKA (PDB code: 1CDK). These structural features are virtually the same as the Rho-kinase-fasudil complex (*15*).

Y-27632 binds to the inter-subdomain cleft where substrate ATP is known to bind, but a significant overlap of atoms is only observed between the pyridine ring of Y-27632 and the adenine moiety of ATP when superposed in the cleft (Fig. 1b and the drug chemical structure in Fig. 4a). Although contacts between Y-27632 and the kinase domain are mainly hydrophobic, two specific polar interactions hold the elongated Y-27632 molecule on both ends (Fig. 2). Deep in the cleft, a hydrogen bond is formed between the main-chain amide group of Met172 and the pyridine nitrogen atom of the inhibitor. On the other end, the terminal amino group forms two hydrogen bonds to the two catalytic residues, Asn219 and Asp232. Interestingly, this amino group is placed almost exactly at the site where Asn219 and Asp232 should hold one of the ATP-associated magnesium ions that bridges the α- and γ-phosphate oxygen atoms (Fig. 1b).

We aligned structures between the Rho-kinase-Y-27632 complex and the three relevant structures reported to

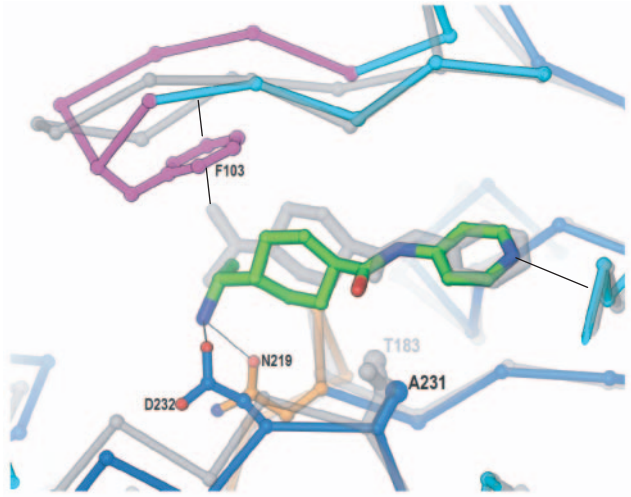

Fig. 2. **Comparison of the Y-27632 molecules bound to Rho-kinase and PKA.** A close-up view from the interior of the cleft. The kinase domains of Rho-kinase and PKA are superposed as in Table 2. The C_α trace of Rho-kinase is shown in purple (P-loop), orange (C-loop), cyan (N lobe) and blue (C lobe), and that of PKA in gray. The side chains of Phe103, Asn219, Asp232 and Ala231 of Rho-kinase are shown. The side chain of PKA Thr183, which is a corresponding residue to Ala231 of Rho-kinase is also shown. Hydrogen bonds are indicated with thin lines. Y-27632 has the terminal amino group hydrogen bonding to Rho-kinase Asn219 and Asp232 with the pyridine ring forming a common hydrogen bond to the main chain of Rho-kinase Met172 (PKA Val123). The flipped terminal amino group of Y-27632 bound to PKA forms an alternative hydrogen bond to the main chain (PKA Thr51) of the P loop.

Table 2. **Structural alignments.**

	PDB code	Molecule	rmsd (Å)	Aligned Cα atoms	Identical residues
PKA–Y-27632	1Q8T		0.81	160	72
ROCK I–Y-27632	2ETR	A	0.50	290	259
		B	0.53	296	264
Rho-kinase-fasudil	2F2U	A	0.54	291	291
		B	0.63	263	263

Each structure was aligned to the Rho-kinase-Y-27632 complex by initial superposition of the C-loop (residues 214–219 in Rho-kinase) and subsequent improvements using the least square fitting algorithm in O with a distance cut-off criteria of 1.5 Å for 5 contiguous residues. The total number of C_α atoms tested for alignment was 323 for Rho-kinase, corresponding to residues 85–417 with deletion of residues 389–398.

date: the PKA-Y-27632 complex (*21*), the human ROCK I-Y-27632 complex (*22*), and the Rho-kinase-fasudil complex (*15*) (Table 2). Compared with PKA, the inhibitor binding site of Rho-kinase contains nonconservative residues, Ile98, Met172, Ala231, Asp176 and Asp218, which are replaced with Leu, Val, Thr, Glu and Glu residues in PKA, respectively. Of these, Asp176 and Asp218, which form hydrogen bonds to fasudil, do not participate in the direct interactions with Y-27632 in either Rho-kinase or PKA.

Ala231 of Rho-kinase and its counter part Thr183 of PKA is located at the interior of the cleft. Differences in the sizes of the side chains of these residues, the bulky side chain of PKA Thr183 and the smaller one of Rho-kinase Ala231

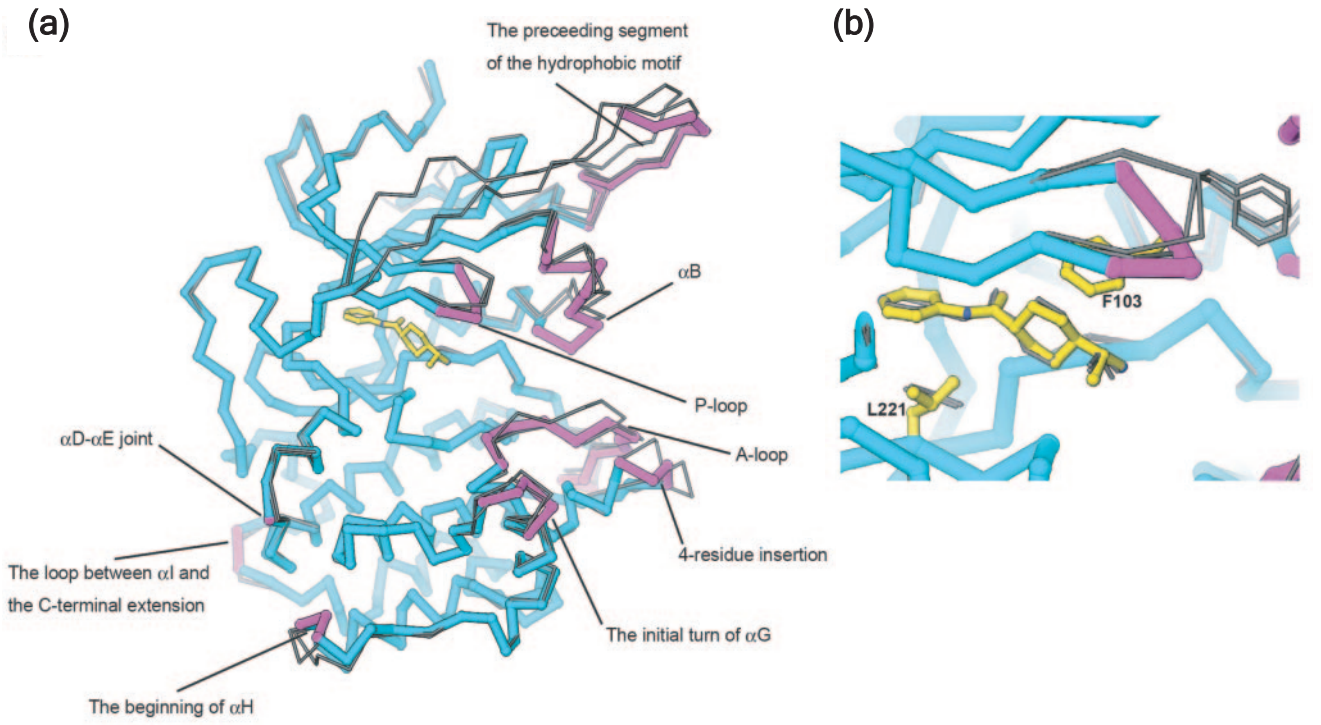

Fig. 3. **Structural differences between Rho-kinase and ROCK I.** (a) The kinase domains of Rho-kinase and ROCK I bound to Y-27632 are superposed. The bound inhibitor is shown as a ball-and-stick model. The C_α traces of ROCK I are shown as thin grey lines. The Rho-kinase C_α trace is shown as thick cyan sticks. Segments that have more than 1.0 Å C_α distances between Rho-kinase and ROCK I are shown in magenta and labeled; the P-loop (residues 101–104), the A-loop (240–254), helix αB (126–135), a 4-residue bulge insertion segment (as against PKA) adjacent to the A-loop (265–268), and helix αG (397–301). The segment comprising residues 399–409 preceding the hydrophobic motif in the C-terminal extension also shows significant deviation. Certain minor changes are seen in junctions between secondary structural elements including the regions between helices αD and αE (residue 185), at the beginning of αH (318–320), and between helix αI and the C-terminal extension (357–358). (b) A close-up view of the Y-27632 binding site. The side chains of residues Phe103 and Leu221 of Rho-kinase are yellow and labeled. The corresponding residues in the ROCK I-Y-27632 complex are shown along with their bound inhibitors as thin grey sticks.

induce a slight but significant difference in orientation of Y-27632 (Fig. 2). The pyridine nitrogen atoms of Y-27632 occupy the same position in Rho-kinase and PKA by forming a common hydrogen bond to the main chain, whereas the rest of the inhibitor bound to PKA is shifted by more than 1 Å toward outside of the cleft by making contacts with the bulky side chain of Thr183. The shift destabilizes the hydrogen bond to Asp183 (Asp232 of Rho-kinase) by being distant from this residue. This results in the disordered conformations of the terminal amino group to have two alternative conformations (*21*). In the alternative conformation, the amino group of Y-27632 flips to form a single hydrogen bond to the main chain of the P-loop (Thr51). Ile98 and Met172 also induce subtle structural variations between Rho-kinase and PKA.

The most significant difference is found in the P-loop conformations (Fig. 2). Like the Rho-kinase P-loop in the fasudil-bound form (Molecule A) (*15*), the Rho-kinase P-loop in the Y-27632-bound form displays an induced-fit conformational change for binding Y-27632, where the loop is folded toward inside with a flip of the Phe103 side chain to increase surface complementarity with the inhibitor. PKA exhibits no such induced-fit in the P-loop. The differences in the P-loop conformations and the Y-27632 positions result in an increased number (33 contacts) of the inhibitor-protein contacts in the Rho-kinase than that (22 contacts) in PKA. These observations could provide the structural basis for the high selectivity of Y-27632.

The Phe103 conformation in our structure might represent an important part of the inhibitor binding mechanism. The very first case of such an induced-fit mechanism of inhibitor binding in the P-loop region was observed in the structure of the FGF receptor cytoplasmic tyrosine kinase domain in complex with the specific inhibitor SU5402 (*23*). This conformational change of the P-loop reflects its flexible nature to function as a flap on the bound substrate ATP. In the Rho-kinase-fasudil complex, the same kind of conformational change in the P-loop was observed in one of the two crystallographically independent molecules. In that case, the inhibitor appears to alter its conformation significantly to accommodate the Phe103 side chain. The overall structures, except for the P-loop region, align best between the Y-27632 complex and the other fasudil complex in which Phe103 does not participate in inhibitor binding. Y-27632 possesses more contacts than fasudil in the Rho-kinase catalytic domain, which might explain the better binding of Y-27632 compared with fasudil.

The Rho-kinase-Y-27632 complex superposes slightly better on the ROCK I-Y-27632 complex than on the

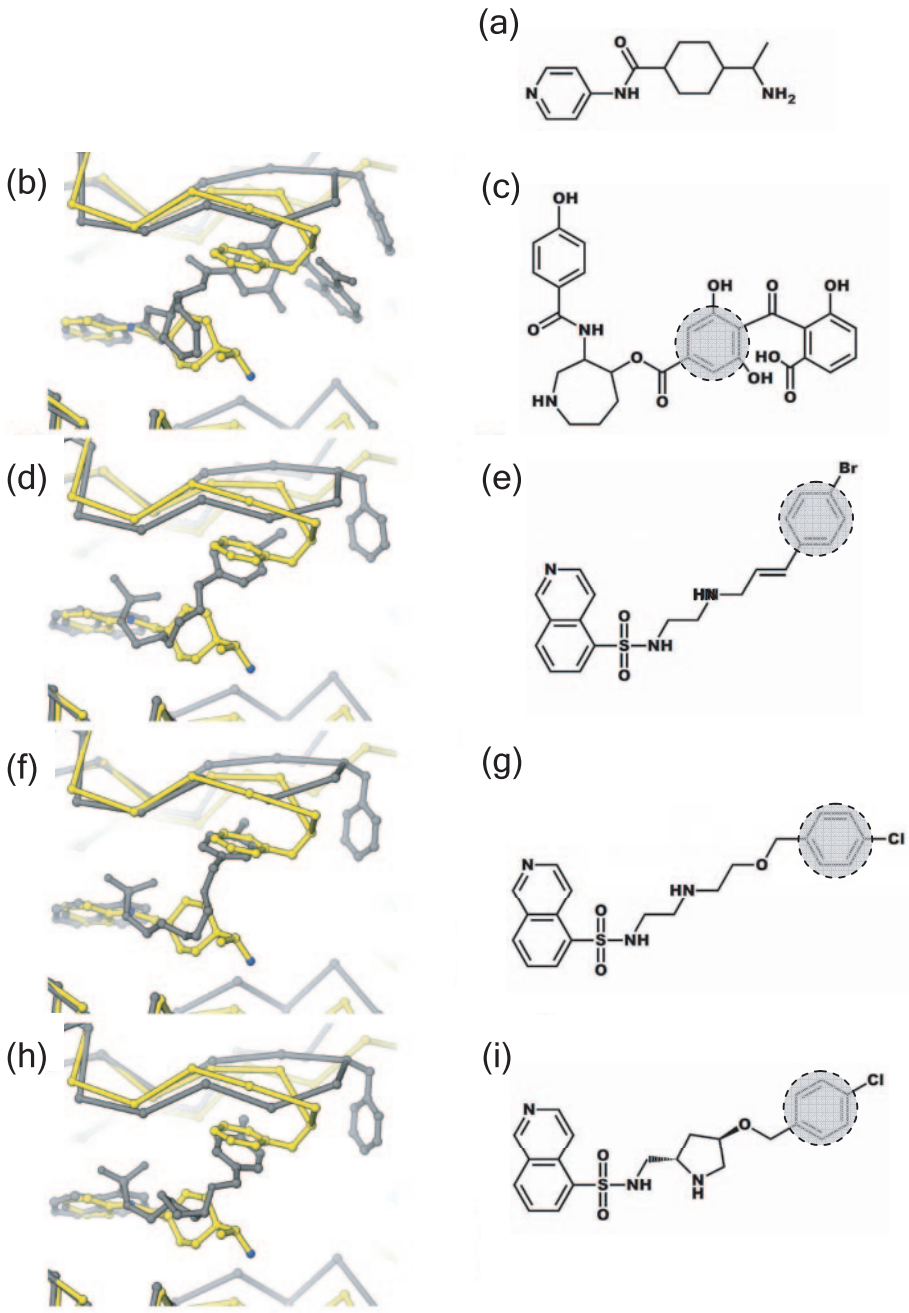

Fig. 4. **Aromatic rings are sheltered underneath the P-loop in some protein kinase inhibitor complexes.** In the Rho-kinase-Y-27632 complex structure, residues were identified as possessing significant interactions with the bound Y-27632, based on calculations using CONTACT in the CCP4 suite. Using LSQMAN (*24*) with the default distance cut-off criteria, 575 eukaryotic protein kinase structures in the PDB were aligned individually on the Rho-kinase-Y-27632 structure. The resulting alignments were sorted in the order of rms distances and number of aligned residues. For further analyses, 27 structures were selected that retained the residues in the alignment: 2ETR (chain A and B), 2ETK (chain A and B), 2ESM (chains A and B), 2ETO (chains A and B), 2C1A (chain A), 1O6L (chain A), 1YDS (chain A), 2ERZ (chain A), 1JLU (chain A), 1O6K (chain A), 1YDR (chain A), 1APM (chain A), 1JPB (chain A), 1YDT (chain A), 2CPK (chain A), 1ATP (chain A), 1BKX (chain A), 1BX6 (chain A), 1FMO (chain A), 2C1B (chain A), 1CDK (chains A and C), 1L3R (chain A). The superposed structures were visually inspected using the program O. The inhibitors are balanol (1BX6), *N*-(2-(3-(4-bromophenyl)allylamino)ethyl)isoquinoline-5-sulfonamide (1YDT), *N*-(2-(2-(4-chlorobenzyloxy)ethylamino)ethyl)isoquinoline-5-sulfonamide (2C1A) and *N*-(((2*S*,4*R*)-4-(4-chlorobenzyloxy)pyrrolidin-2-yl)methyl)isoquinoline-5-sulfonamide (2C1B). Except for balanol, these inhibitors are structurally related in that they possess two aromatic rings, an isoquinoline ring and a halogenated benzene ring, connected by 8- or 9-atom spacers. (a) Chemical structure of the Rho-kinase-specific inhibitor Y-27632. (b) Superposition of the structures between the Rho-kinase-Y-27632 complex (yellow) and the PKA-balanol complex (PDB code: 1BX6; grey) with the chemical structure of balanol in (c). The Cα traces and the bound inhibitors are shown as ball-and-stick models. The aromatic ring that is located at the pocket for Phe103 is highlighted with a circle. (d) Same as in (b) for the PKA-*N*-(2-(3-(4-bromophenyl)allylamino)ethyl)isoquinoline-5-sulfonamide complex (PDB code: 1YDT) with the chemical structure of the inhibitor in (e). (f) Same as in (b) for the PKA-*N*-(2-(2-(4-chlorobenzyloxy)ethylamino)ethyl)isoquinoline-5-sulfonamide complex (PDB code: 2C1A) with the chemical structure of the inhibitor in (g). (h) Same as in (b) for the PKA-*N*-((((2*S*,4*R*)-4-(4-chlorobenzyloxy)pyrrolidin-2-yl)methyl)isoquinoline-5-sulfonamide complex (PDB code: 2C1B) with the chemical structure of the inhibitor in (i). The aromatic ring that occupies the same position as the Phe103 side-chain in the Rho-kinase-Y-27632 complex is indicated by a grey circle in (c), (e), (g) and (i).

Rho-kinase-fasudil complex, even though ca. 10% of the aligned residues between Rho-kinase and ROCK I are not identical (Table 2). This implies that a structural adaptation following inhibitor binding can significantly affect the overall conformation of the protein kinase. Local structural differences between Rho-kinase and ROCK I are found in loop regions including the P-loop (residues 101–104), helix αB (residues 126–135) and the segment comprising residues 399–409 preceding the hydrophobic motif in the C-terminal extension (Fig. 3a). Of the differences

observed in side-chain conformations between Rho-kinase and ROCK I, those of Phe103 and Leu221 seem relevant to inhibitor binding (Fig. 3b). As mentioned above, the P-loop in our Rho-kinase structure has a so-called 'folded' conformation with the side-chain phenyl group of Phe103 that is turned inward and is sandwiched between the P-loop and the bound Y-27632 molecule. Contrary to this, the corresponding phenyl ring in ROCK I is projected outward and stabilized through hydrophobic interactions with the methionine and phenylalanine residues in helix αB. The absence of these interactions in our Rho-kinase might be cause of flexibility in helix αB. In Rho-kinase, Leu221 comprises part of the hydrophobic stage for binding to the aromatic rings of substrate ATP as well as inhibitor molecules. While it maintains the most favorable rotamer conformation, the equivalent residue in ROCK I, Leu205, shows one of the most unfavorable conformations. This difference was also observed between our previously reported Rho-kinase-fasudil complex and the PKA-fasudil complex structures. The number of van der Waals contacts with the bound ligand is increased in the stable rotamer of the Rho-kinase, because of the protruding terminal methyl groups. This might simply reflect differences in the binding affinity.

Other kinases that might possess similar modes of kinase-inhibitor complex formation as that found in the Rho-kinase-Y-27632 complex were then sought. To this end, 575 protein kinase structures in the Protein Data Bank (PDB) were individually superposed to our Rho-kinase structure by least square fitting of the corresponding residues involved in Y-27632 binding to Rho-kinase. Structures with rms Cα distances less than 0.6 Å were examined further. As expected, the best aligned were those structures of ROCK I, although several structures of PKA in complex with various inhibitors also stood out. Four inhibitors (PDB codes: 1BX6, 1YDT, 2C1A and 2C1B) bind to PKA with their aromatic rings in virtually the same position as that occupied by the Phe103 side chain in our Rho-kinase-Y-27632 complex (Fig. 4). This suggests the presence of a pocket beneath the phosphate-binding loop that favors binding of a small aromatic ring. Except for balanol (Fig. 4, b and c), these inhibitors are structurally related in that they possess two aromatic rings, an isoquinoline ring and a halogenated benzene ring, connected by 8- or 9-atom spacers.

The structure of the Rho-kinase-Y-27632 complex showed a closed "active" conformation even without phosphorylation of the activation loop. The overall conformation of Rho-kinase seems to be dictated by the bound inhibitor that affects the relative position of contact residues within the interlobal cleft. The intrinsic flexibility of the phosphate-binding loop facilitates a conformational change to a "folded" form. To date, no physiological role has been associated with the flip-in/flip-out motion of the phenyl ring at the tip of the P-loop in our structure. However, it is certain that additional stability is gained during Y-27632 binding by an induced-fit conformational change in Rho-kinase. This might represent yet another case of induced-fit binding in protein kinases. The conserved Phe103 at the tip of the phosphate-binding loop rotates its side-chain phenyl group and interleaves the loop and bound ligand. Such placement of the Phe103 side-chain might encourage the development of novel modification schemes of current protein kinase inhibitors. By modifying Y-27632 to introduce an additional aromatic ring that can occupy the corresponding site to the Phe103 side-chain, more stable binding can be achieved while maintaining the natural conformation of the P-loop in Rho-kinase.

The atomic coordinates and structure factors (code 2H9V) has been deposited in the Protein Data Bank, Research Collaboratory for Structural Bioinformatics, Rutgers University, New Brunswick, NJ. We thank J. Tsukamoto for her technical support in performing MALDI-TOF MS and the N-terminal analysis, Drs. T. Tsukihara, A. Nakagawa, and E. Yamashita at SPring-8 for use of the synchrotron beamline BL44XU. This work was supported in part by a Protein 3000 project on Signal Transduction from the Ministry of Education, Culture, Sports, Science and Technology (MEXT) of Japan (to T. H.)

REFERENCES

1. Leung, T., Manser, E., Tan, L., and Lim, L. (1995) A novel serine/threonine kinase binding the Ras-related RhoA GTPase which translocates the kinase to peripheral membranes. *J. Biol. Chem.* **270**, 29051–29054
2. Ishizaki, T., Maekawa, M., Fujisawa, K., Okawa, K., Iwamatsu, A., Fujita, A., Watanabe, N., Saito, Y., Kakizuka, A., Morii, N., and Narumiya, S. (1996) The small GTP-binding protein Rho binds to and activates a 160 kDa Ser/Thr protein kinase homologous to myotonic dystrophy kinase. *EMBO J.* **15**, 1885–1893
3. Kimura, K., Ito, M., Amano, M., Chihara, K., Fukata, Y., Nakafuku, M., Yamamori, B., Feng, J., Nakano, T., Okawa, K., Iwamatsu, A., and Kaibuchi, K. (1996) Regulation of myosin phosphatase by Rho and Rho-associated kinase (Rho-kinase). *Science* **273**, 245–248
4. Matsui, T., Amano, M., Yamamoto, T., Chihara, K., Nakafuku, M., Ito, M., Nakano, T., Okawa, K., Iwamatsu, A., and Kaibuchi, K. (1996) Rho-associated kinase, a novel serine/threonine kinase, as a putative target for small GTP binding protein Rho. *EMBO J.* **15**, 2208–2216
5. Peterson, R.T. and Schreiber, S.L. (1999) Kinase phosphorylation: Keeping it all in the family. *Curr. Biol.* **9**, R521–524
6. Pearl, L.H. and Barford, D. (2002) Regulation of protein kinases in insulin, growth factor and Wnt signalling. *Curr. Opin. Struct. Biol.* **12**, 761–767
7. Newton, A.C. (2003) Regulation of the ABC kinases by phosphorylation: protein kinase C as a paradigm. *Biochem. J.* **370**, 361–371
8. Leung, T., Chen, X.Q., Manser, E., and Lim, L. (1996) The p160 RhoA-binding kinase ROK alpha is a member of a kinase family and is involved in the reorganization of the cytoskeleton. *Mol. Cell. Biol.* **16**, 5313–5327
9. Fukata, Y., Amano, M., and Kaibuchi, K. (2001) Rho-Rho-kinase pathway in smooth muscle contraction and cytoskeletal reorganization of non-muscle cells. *Trends Pharmacol. Sci.* **22**, 32–39
10. Mueller, B.K., Mack, H., and Teusch, N. (2005) Rho kinase, a promising drug target for neurological disorders. *Nat. Rev. Drug Discov.* **4**, 387–398
11. Hu, E. and Lee, D. (2005) Rho kinase as potential therapeutic target for cardiovascular diseases: opportunities and challenges. *Expert Opin. Ther. Targets* **9**, 715–736
12. Ono-Saito, N., Niki, I., and Hidaka, H. (1999) H-series protein kinase inhibitors and potential clinical applications. *Pharmacol. Ther.* **82**, 123–131
13. Uehata, M., Ishizaki, T., Satoh, H., Ono, T., Kawahara, T., Morishita, T., Tamakawa, H., Yamagami, K., Inui, J., Mae-

kawa, M., and Narumiya, S. (1997) Calcium sensitization of smooth muscle mediated by a Rho-associated protein kinase in hypertension. *Nature* **389**, 990–994
14. Davies, S.P., Reddy, H., Caivano, M., and Cohen, P. (2000) Specificity and mechanism of action of some commonly used protein kinase inhibitors. *Biochem. J.* **351**, 95–105
15. Yamaguchi, H., Kasa, M., Amano, M., Kaibuchi, K., and Hakoshima, T. (2006) Molecular mechanism for the regulation of rho-kinase by dimerization and its inhibition by fasudil. *Structure* **14**, 589–600
16. Otwinowski, Z. and Minor, W. (1997) Processing of X-ray diffraction data collected in oscillation mode in *Methods in Enzymology* (Charles, J. and Carter W., eds.) Vol. 276, pp. 307–326, Academic Press, New York
17. Collaborative Computational Project, Number 4 (1994) The CCP4 suite: programs for protein crystallography. *Acta Crystallogr. D Biol. Crystallogr.* **50**, 760–763
18. Kleywegt, G.J. and Jones, T.A. (1997) Model building and refinement practice, in *Methods in Enzymology* (Carter Jr., C.W. and Sweet, R.M. eds.) Vol. 277, pp. 208–230, Academic Press, New York
19. Murshudov, G.N., Vagin, A.A., Lebedev, A., Wilson, K.S., and Dodson, E.J. (1999) Efficient anisotropic refinement of macromolecular structures using FFT. *Acta Crystallogr. D Biol. Crystallogr.* **55**, 247–255
20. Laskowski, R.A., MacArthur, M.W., Moss, D.S., and Thornton, J.M. (1993) PROCHECK: a program to check the stereochemical quality of protein structures. *J. Appl. Crystallogr.* **26**, 283–291
21. Breitenlechner, C., Gassel, M., Hidaka, H., Kinzel, V., Huber, R., Engh, R.A., and Bossemeyer, D. (2003) Protein kinase A in complex with Rho-kinase inhibitors Y-27632, Fasudil, and H-1152P: structural basis of selectivity. *Structure* **11**, 1595–1607
22. Jacobs, M., Hayakawa, K., Swenson, L., Bellon, S., Fleming, M., Taslimi, P., and Doran, J. (2006) The structure of dimeric ROCK I reveals the mechanism for ligand selectivity. *J. Biol. Chem.* **281**, 260–268
23. Mohammadi, M., McMahon, G., Sun, L., Tang, C., Hirth, P., Yeh, B.K., Hubbard, S.R., and Schlessinger, J. (1997) Structures of the tyrosine kinase domain of fibroblast growth factor receptor in complex with inhibitors. *Science* **276**, 955–960
24. Kleywegt, G.J. (1996) Use of non-crystallographic symmetry in protein structure refinement. *Acta Crystallogr. D Biol. Crystallogr.* **52**, 842–857